Wu et al. Virology Journal (2025) 22:56
https://doi.org/10.1186/s12985-025-02673-2

Virology Journal

RESEARCH Open Access

Mycophenolate mofetil exerts broad-spectrum antiviral activity against coronaviruses including SARS-CoV-2

Mengyuan Wu[1], Kun Wang[1], Huiqiang Wang[1], Haiyan Yan[1], Shuo Wu[1,2], Ge Yang[1], Yuhuan Li[2*], Yongsheng Che[2*] and Jiandong Jiang[2*]

Abstract

Background New anti-coronavirus drugs are continuously being developed to address the serious long-term challenge posed by numerous SARS-CoV-2 variants. The clinical immunosuppressants mycophenolate mofetil (MMF) and mycophenolic acid (MPA) have been reported to have anti-coronavirus activities. However, systematic studies have not been conducted to evaluate their activities and mechanisms against pan-coronaviruses, including SARS-CoV-2.

Methods The antiviral effect of MMF and MPA was determined by qRT-PCR assay, Western blotting, and immunofluorescence assay. The IMPDH inhibition effect of MMF was determined by cellular thermal shift assay and Western blotting.

Results We showed that MMF and MPA had broad-spectrum inhibitory effect against coronavirus, including HCoV-229E, HCoV-OC43, and SARS-CoV-2 ancestral strain and its variants. In terms of characteristics, MMF acted in the early stages of viral infection and inhibited viral replication by blocking purine nucleotide synthesis through interaction with inosine-5′-monophosphate dehydrogenase (IMPDH). Therefore, the antiviral effect of MMF can be reversed by exogenous guanosine. Additionally, MMF in combination with molnupiravir, GC376 or E64d showed synergistic antiviral effects.

Conclusion MMF and MPA exerted broad-spectrum anti-coronavirus effects by inhibiting IMPDH activity. MMF had a synergistic antiviral effect when combined with other drugs, showing its potential clinical antiviral applications.

Keywords MMF, MPA, Coronavirus, SARS-CoV-2, IMPDH, Drug combination

*Correspondence:
Yuhuan Li
yuhuanlibj@126.com
Yongsheng Che
cheys@im.ac.cn
Jiandong Jiang
jiang.jdong@163.com
[1] CAMS Key Laboratory of Antiviral Drug Research, Beijing Key Laboratory of Technology and Application for Anti-Infective New Drugs Research and Development, NHC Key Laboratory of Biotechnology of Antibiotics, Institute of Medicinal Biotechnology, Chinese Academy of Medical Sciences and Peking Union Medical College, Beijing, China
[2] State Key Laboratory of Bioactive Substances and Functions of Natural Medicines, Institute of Medicinal Biotechnology, Chinese Academy of Medical Sciences and Peking Union Medical College, Beijing 100050, China

Background

Coronaviruses (CoVs) are enveloped, single-stranded, positive-sense RNA viruses belonging to the Coronaviridae family. They are classified into four genera, namely, *Alpha* (α), *Beta* (β), *Delta* (δ), and *Gamma* (γ) [1]. CoVs have a wide host spectrum and are prone to interspecies transmission [2]. Currently, seven CoVs are known to infect humans, the common cold CoVs HCoV-229E, HCoV-OC43, HCoV-NL63, and HCoV-HKU1, as well as the highly pathogenic SARS-CoV, MERS-CoV, and SARS-CoV-2 [3]. Since COVID-19 outbreak at the end of 2019, a worldwide health crisis ensued, with 7 million deaths among more than 776.8 million confirmed cases as of November 2024 (WHO, 2024). Several specific antiviral drugs including Paxlovid (nirmatrelvir/ritonavir), Lagevrio (molnupiravir), Veklury (remdesivir) and Azvudine, which targeted the main protease or the RNA-dependent RNA polymerase (RdRp), have been approved by the FDA, EMA, or NMPA [4–6]. However, the continuous emergence of SARS-CoV-2 variants not only causes immune escape, rendering vaccines and antibodies ineffective, but also leads to severe illness, especially in elderly or comorbid patients [7, 8]. And it can also cause resistance to small molecule antiviral drugs [9]. So, it will be important to develop novel strategies to inhibit virus infection and thus combat the disease.

Mycophenolic acid (MPA) is a secondary metabolite synthesized by the filamentous fungus *Penicillium roqueforti*, which belongs to genus *Penicilllium*. Mycophenolate mofetil (MMF) is the 2-morpholinoethyl ester of MPA, which is chemically engineered and has enhanced bioavailability and absorption [10]. MMF and MPA are generally served as immunosuppressants in clinical practice to prevent the immune system from attacking and rejecting transplanted organs [11]. Additionally, MMF and MPA are also used in the daily treatment of autoimmune diseases, skin diseases, rheumatoid arthritis, systemic lupus erythematosus, and nephrotic syndrome [12, 13]. As reversible non-competitive inosine-5′-monophosphate dehydrogenase (IMPDH) inhibitors, MMF and MPA inhibit the synthesis of guanosine triphosphate in the de novo purine synthesis pathway, thereby specifically inhibiting the proliferation and activation of rapidly proliferating lymphocytes to inhibit immune system [14, 15].

MMF and MPA reportedly have antiviral activities, toward MERS-CoV, influenza A virus, dengue virus, Zika virus, coxsackie B3 virus, and Mpox virus [16–21]. Their potential mechanisms are related to inhibiting IMPDH activity [22], stimulating the expression of interferon-stimulated genes (ISGs) [23], and suppressing autophagy [24, 25]. Recent studies have also shown that MMF and MPA have potential anti-SARS-CoV-2 activities [26, 27], but systematic studies on related efficacy and mechanisms are still lacking. Therefore, the anti-CoVs activity of MMF is worthy of further research.

In the present study, we systematically studied the anti-CoVs activities and characteristics of MMF and MPA and subsequently explored the combined antiviral effects of MMF and other drugs. Our results can provide strong theoretical support for the clinical applications of MMF and MPA in the treatment of CoVs infection.

Methods

Cells and viruses

Human hepatocellular carcinoma cell lines Huh7 and Huh7.5 were provided by Dr. Zonggen Peng [28]. Human lung cancer cell line H460 was provided by Dr. Zhen Wang [29]. They are both from the Institute of Medicinal Biotechnology, Chinese Academy of Medical Sciences. Human hepatoblastoma cell line C3A was purchased from American Type Culture Collection (ATCC, Manassas, VA, USA). African green monkey kidney cell line Vero E6 was provided by the Institute of Medical Biology, Chinese Academy of Medical Sciences (Yunnan, China) [30]. Human lung adenocarcinoma cell line Calu-3 was purchased from the Institute of Basic Medical Sciences, Chinese Academy of Medical Sciences (Beijing, China). Human nasal septal squamous carcinoma cell RPMI-2650 was purchased from GuangZhou Jennio Biotech Co.,Ltd (Guangzhou, China). All cells cultured with supplementation of 10% fetal bovine serum and antibiotics (100 U/mL penicillin and 100 mg/mL streptomycin) at 37 °C in a 5% CO_2 incubator. All cells were detected mycoplasma regularly to confirm the cells were free of mycoplasma contamination. Huh7, Huh7.5, H460, and Vero E6 cells were cultured in Dulbecco's modified eagle medium (DMEM, Invitrogen, Carlsbad, CA, USA), C3A and RPMI-2650 cells were cultured in minimum essential medium (MEM, Invitrogen), Calu-3 cells were cultured in Roswell Park Memorial Institute-1640 medium (RPMI-1640, Invitrogen).

HCoV-229E (strain VR740) was purchased from ATCC. HCoV-OC43 (strain VR1558) was provided by Dr. Xuesen Zhao at Beijing Ditan Hospital, Capital Medical University (Beijing, China) [31]. The SARS-CoV-2 ancestral strain (wild type, WT), alpha variant (B.1.1.7), beta variant (B.1.351), and omicron variants (BA.5, EG.5, and XBB.1.16) were provided by the Institute of Medical Biology, Chinese Academy of Medical Sciences (Yunnan, China).

Compounds

MMF was purchased from Hiboled century (Shenzhen, China). MPA was purchased from Macklin (Shanghai, China). Remdesivir (RDV) and molnupiravir were

purchased from Med Chem Express (Monmouth Junction, NJ, USA). Ribavirin (RBV) and guanosine were purchased from Sigma Aldrich (St. Louis, MO, USA). GC376 and E64d were purchased from TOP SCIENCE (Shanghai, China).

Cytotoxicity assay

Cytotoxic effects of MMF and MPA on different cell lines were assayed with a cell-counting kit (CCK; TransGen Biotech, Beijing, China). In a typical procedure, cells (2.5×10^4 cells/well) were seeded onto 96-well culture plates and incubated overnight. Cells were then treated with different concentrations of MMF and MPA for 24 h. Subsequently, 10 μL of CCK solution was added and incubated for 60 min. The optical density was measured at 450 nm in a Victor X5 Plate Reader (PerkinElmer, Waltham, MA, USA). The half-maximal toxic concentration (TC_{50}) was calculated by GraphPad Prism 7.0 software (GraphPad Software Inc.).

Quantitative reverse-transcription (qRT) polymerase chain reaction (PCR) assay

Cells (2.5×10^5 cells/well) were seeded onto 12-well culture plates and incubated overnight. Infection was performed at multiplicity of infection (MOI) of 0.35 for HCoV-229E and HCoV-OC43, and MOI of 0.05 or 0.09 for SARS-CoV-2 for 24 h. The total RNA of the infected cells was extracted using the RNeasy Mini Kit (QIAGEN, Hilden, Germany) according to the manufacturer's instructions. qRT-PCR was performed with a One-Step qRT-PCR Kit (TransGen Biotech) using the ABI 7500 Fast Real-Time PCR system (Applied Biosystems). The comparative threshold method was performed for relative quantification. Firstly, the CT values of target gene were subtracted from that of housekeeping gene GAPDH to obtain the $\triangle$CT, and then the $\triangle$CT of each experimental group was subtracted from that of the control group to obtain the $\triangle\triangle$CT. Finally, the values of $2^{(-\triangle\triangle CT)}$ was used as the final result. The applied primer sequences are shown in Table 1. IC_{50} (half maximal inhibitory concentration) was calculated using GraphPad Prism 7.0 software (GraphPad Software Inc.), according to qRT-PCR assay. The selectivity index was the quotient of TC_{50} and IC_{50}.

Western blotting

Cells (2.5×10^5 cells/well) were seeded onto 12-well culture plates and incubated overnight. Infection was performed at MOI of 0.35 for HCoV-229E and HCoV-OC43 for 24 h. Cells were collected and cellular proteins were extracted using Mammalian Protein Extraction Reagent (Thermo Fisher, Waltham Mass, USA) with halt protease inhibitor for 30 min. Centrifugation was conducted at 12,000 rpm at 4 °C for 20 min, and the supernatant was mixed with loading buffer. The supernatant was boiled in a metal bath at 100 °C for 10 min and then subjected to sodium dodecyl sulfate–polyacrylamide gel electrophoresis (SDS-PAGE). The electrophoresis products were transferred onto a 0.22 μM polyvinylidene fluoride (PVDF) film, and PVDF membranes were incubated with specific primary antibody and horse radish peroxidase (HRP)-labeled secondary antibody of different species. The primary antibodies used were antibodies against glyceraldehyde-3-phosphate dehydrogenase (Cell Signaling Technology, Boston, MA, USA, 1:1000), HCoV-229E NP (Sino Biological, Beijing, China, 1:8000), HCoV-OC43 nucleocapsid protein (NP; Millipore, Billerica, MA, USA,1:1000), and IMPDH2 (Abcam, Cambridge, UK, 1:1000). The secondary antibody included anti-rabbit and anti-mouse HRP-labeled antibodies (Cell Signaling Technology, 1:5000). The expression levels of each target protein and internal reference GAPDH were defined with Image J software based on grayscale values.

Table 1 Primers used in qRT-PCR assay

Primer	Sequence(5′→3′)
HCoV-229E *NP* Sense	CGCAAGAATTCAGAACCAGAG
HCoV-229E *NP* Antisense	GGCAGTCAGGTTCTTCAACAA
GAPDH (human) Sense	CTCTGGAAAGCTGTGGCGTGATG
GAPDH (human) Antisense	ATGCCAGTGAGCTTCCCGTTCAG
HCoV-OC43 *NP* Sence	CGATGAGGCTATTCCGACTAGGT
HCoV-OC43 *NP* Antisense	CCTTCCTGAGCCTTCAATATAGTAACC
HCoV-OC43 *NP* Probe	TAMRA-TCCGCCTGGCACGGTACTCCCT-BHQ2
GAPDH (human) Sense	CGGAGTCAACGGATTTGGTCGTAT
GAPDH (human) Antisense	AGCCTTCTCCATGGTGGTGAAGAC
GAPDH (human) Probe	TAMRA- CCGTCAAGGCTGAGAACGG -BHQ2
IFN-α Sense	CTGTCCTCCATGAGATGATCC
IFN-α Antisense	CTCATGATTTCTGCTCTGACAACC
IFN-β Sense	GCTGGAATGAGACTATTGTTGAGA
IFN-β Antisense	CAGTTTCGGAGGTAACCTGTAAG

Virus titer assay

RPMI-2650 cells (2.5×10^5 cells/well) were seeded onto 12-well culture plates and incubated overnight. Infection was performed at MOI of 0.35 for HCoV-229E and HCoV-OC43. Cells were harvested 24 h.p.i., following a single freeze–thaw cycle to release intracellular virus particles. The cells were centrifuged at 3000 rpm at 4 °C for 30 min to remove cellular debris, and the supernatant was collected for determine viral titers based on cytopathic effect (CPE) reduction assays. Huh7.5 cells were used for HCoV-229E observed 72 h.p.i and H460 cells were used for HCoV-OC43 observed 96 h.p.i. Viral titers

were calculated using the 50% tissue culture infectious dose ($TCID_{50}$) assay, according to the Reed and Muench method [32].

Immunofluorescence (IF) assay

Cells (2.5×10^4 cells/well) were seeded onto 96-well culture plates and incubated overnight. Cells were then infected at MOI of 0.35 for HCoV-229E and HCoV-OC43. IF-staining experiments were performed 24 h after infection. We added 4% paraformaldehyde and incubated the plates at room temperature for 15 min to fix them. Enhanced immunostaining permeabilization buffer (Beyotime Institute of Biotechnology, Shanghai, China) was added and incubated at room temperature for 20 min. Rapid block buffer (Beyotime Institute of Biotechnology) was added and incubated at room temperature for 1 h. A primary antibody recognizing viral double-strand RNA (dsRNA; SCICONS, Szirák, Hungary, 1:200), HCoV-OC43 NP (Millipore, 1:200), or HCoV-229E NP (Sino Biological, 1:200) was added and incubated at room temperature for 1 h or at 4 °C overnight. AF488 conjugate goat anti-rabbit or anti-mouse secondary antibody (TransGen Biotech, 1:200) was added, incubated for 1 h at room temperature, and sheltered from light. Hoechst 33,342 (Beyotime Institute of Biotechnology, 1:100) was added and incubated at room temperature for 30 min. The treated cells were washed with PBS for three times between the above operations. The 96-well plates were photographed using a fluorescence microscope (ZEISS Zen).

Cellular thermal shift assay (CETSA)

Cells (3×10^6 cells/flask) were seeded onto T-75 flasks and incubated overnight. Cells were first collected using cell scrapers in PBS containing protease inhibitors and then lysed by three freezing–thawing cycles. The supernatants were collected after centrifugation at 12,000 rpm and 4 °C and then incubated with MMF or DMSO for 30 min at room temperature, followed by a metal bath at 47, 52, 57, 62, 67, 72, 77, and 82 °C for 3 min to degrade the target proteins. Finally, the supernatants were centrifuged at 12,000 rpm at 4 °C, and the loading buffer was added. The protein samples were prepared by boiling at 100 °C for 10 min. The expression of IMPDH in the two groups incubated with MMF or DMSO was then detected by western blotting. The expression levels of IMPDH were defined with Image J software based on grayscale values.

Time-of-addition assay

A time-of-addition study was performed to dissect the stage of the viral replication that is affected by MMF. Cells (2.5×10^4 cells/well) were seeded onto 96-well culture plates and incubated overnight. Then cells were infected at MOI of 3.5 for HCoV-229E and HCoV-OC43 for 1 h on ice, and 5 μM MMF was added simultaneously for the co-treatment assay (0 h). Cells were washed with PBS and replaced with medium, and the plate was transferred to the 35 °C with 5% CO_2 incubator. For the post-treatment assay, MMF was added at 1, 2, 3, 4, 5,6,7,8 or 9 h after infection, as described in Fig. 5a. Cells were harvested at 9 h and the viral N protein was detected by IF assay.

Statistics analysis

Statistical analyses were performed using GraphPad Prism 7.0 software (GraphPad Software Inc.). Image J software (Rawak Software Inc.) was used for quantitative study on Western blotting data. Results are expressed as the mean ± standard deviation (SD). Data were analyzed by one-way ANOVA, which was divided into "*", "**", and "***", representing " $P<0.05$", " $P<0.01$", and " $P<0.001$", respectively.

Results

MMF and MPA inhibited replication of HCoV-229E and HCoV-OC43

To ensure that the antiviral effect of MMF or MPA (Fig. 1a) was not caused by cytotoxicity to cells, we first determined the cytotoxicity by CCK assay. As shown in Fig. 1b,c, MMF and MPA showed low toxicity to several cell lines, with TC_{50} values above 100 μM.

To systematically study the antiviral effects of MMF and MPA against CoVs, we selected genus *α* (HCoV-229E) and *β* (HCoV-OC43), which were the genera of CoVs that infected humans, as representatives of common cold CoVs for antiviral efficacy testing. NP is the most abundant and conserved protein in CoVs [33], so we targeted NP and detected its transcription and translation levels. The cells were harvested at 24 h post-infection, and mRNA levels of *NP* was tested by qRT-PCR assay. As shown in Fig. 2a–f, MMF and MPA inhibited the RNA levels of HCoV-229E and HCoV-OC43 in a dose-dependent manner in various cell lines. Next, we stained dsRNA, a pivotal intermediate during viral replication, as a complementary indicator of the antiviral properties at the RNA level. We also found that MMF and MPA reduced dsRNA production in cytoplasm (Fig. 2g–j). As shown in Table 2, through further quantitative analysis, it was found that the IC_{50}s of MPA and MMF were both below 0.6 μM in different cells, indicating that their antiviral effects were not cell-specific. In addition, in RPMI-2650 cells sensitive to both HCoV-229E and HCoV-OC43, the IC_{50}s of MPA and MMF against HCoV-OC43 were lower than that of HCoV-229E, suggesting that the anti-CoVs activity of MPA and MMF was certain strain specific.

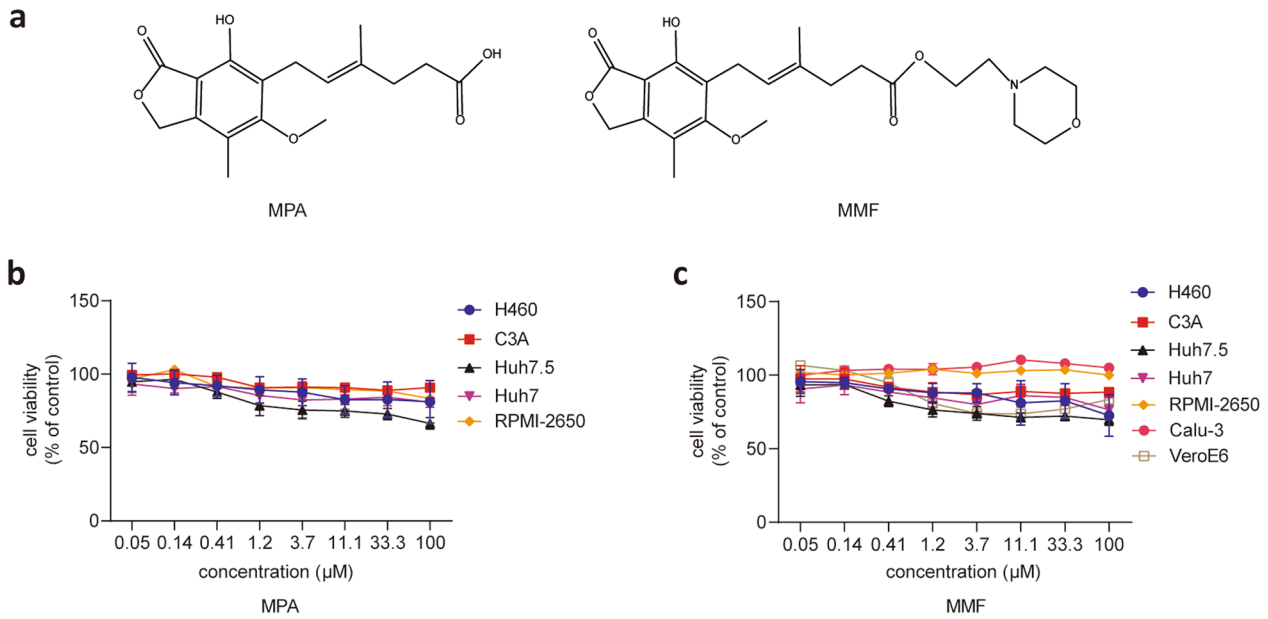

Fig. 1 The chemical structure of compounds and CCK assay. **a** The chemical structures of MPA and MMF. **b** The cytotoxicity of MPA was determined by CCK assay ($n=3$). **c** The cytotoxicity of MMF was determined by CCK assay ($n=3$)

To further investigate whether MMF and MPA had similar antiviral effects at the protein level, Western blotting and IF were used to detect the effects of MMF and MPA on NP protein levels. Unsurprisingly, the Western blotting and IF results were consistent, showing that MMF and MPA inhibited the NP protein levels of HCoV-229E and HCoV-OC43 in a dose-dependent manner in different cells (Fig. 3a–f). The inhibitory effect was more visually demonstrated by IF staining, as shown in Fig. 3g–j. Moreover, MMF and MPA also reduced the levels of progeny HCoV-229E and HCoV-OC43 production (Fig. 3k, l). These results indicated that MMF and MPA exerted promising inhibitory effects on common CoVs.

MMF inhibited various SARS-CoV-2 variants

We further explored the antiviral effects of MMF against SARS-CoV-2, including WT and various variants. Vero E6 cells were infected with SARS-CoV-2 WT, variants B.1.1.7, or B.1.351 (MOI = 0.05), respectively, and treated with MMF for 24 h. As shown in Fig. 4a–c, 1.1 μM MMF inhibited viral replication by up to 90% at the *NP* RNA level. With the mutant strain omicron prevalent and becoming variants of concern, the inhibitory effect of MMF was tested. Similarly, Calu-3 cells were infected with SARS-CoV-2 variants BA.5, EG.5, and XBB.1.16 (MOI = 0.09) and treated with MMF for 24 h. Results revealed that MMF also significantly inhibited delta and omicron variants by more than 50% (Fig. 4d–f). All these results demonstrated that MMF exhibited inhibitory effects on the tested SARS-CoV-2 variants, suggesting its potential to challenge the threat posed by the constantly mutating SARS-CoV-2.

MMF played an antiviral role by inhibiting IMPDH

To explore the antiviral characteristics, we performed the time-of-addition assay to map the viral replication step targeted by MMF. As shown in Fig. 5a–c, treatment before 5 h seemed to be the effective window of MMF, indicating that MMF acted primarily during the early-replication events. Then, we examined whether MMF exhibited antiviral activities through the non-competitive inhibition of IMPDH enzymes. First, CETSA results showed that MMF interacted directly with IMPDH and increased its thermostability in Huh7.5 cells and H460 cells (Fig. 5d, e). Second, we replenished the depleted GTP pool by exogenously adding guanosine simultaneously with virus infection and administration to reverse the inhibitory effects on IMPDH enzyme. Accordingly, changes in the antiviral effects of MMF were evaluated. As shown in Fig. 5f, g, we found that 400 μM guanosine treatment did not affect the replication of HCoV-229E and HCoV-OC43. However, guanosine treatment had a dose-dependent reversal of the antiviral effects of MMF on HCoV-229E and HCoV-OC43, and 400 μM guanosine treatment can completely reverse the antiviral effects of MMF. These results suggested that MMF played an indirect antiviral role by targeting IMPDH. Besides, it was found that MMF pre-treatment also showed antiviral effects without significantly activating interferon

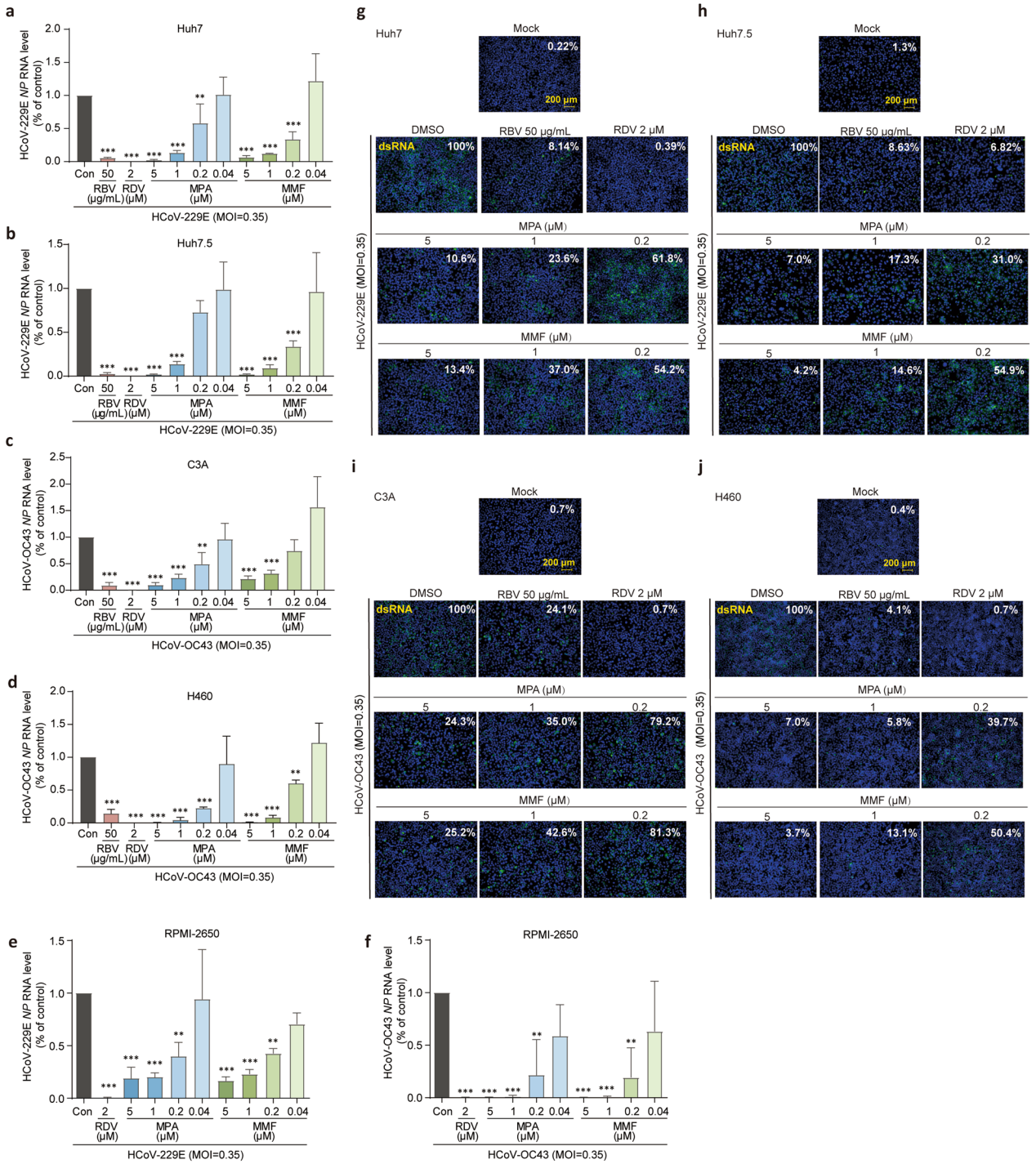

Fig. 2 MMF and MPA inhibited viral RNA levels of HCoV-229E and HCoV-OC43. Cells were infected with HCoV-229E (MOI = 0.35) or HCoV-OC43 (MOI = 0.35), and treated with different concentrations of MMF or MPA for 24 h. **a–f** The cells were harvested for qRT-PCR assay with specific primers, relative quantification was performed and normalized to the housekeeping gene GAPDH ($n = 3$). *$P < 0.05$, **$P < 0.01$, ***$P < 0.001$ *vs.* virus control (Con), one-way ANOVA with Holm-Sidak multiple comparisons test. **g–j** The cells were fixed and intracellular viral double strand RNA (dsRNA) was detected with immunofluorescence (IF) assay. Green particles represent dsRNA and the blue ones represent cell nucleus. The quantitative study on immunofluorescence was comparison of the total fluorescence values of each experimental group with the control group and analyzed by Image J software

Table 2 Anti-coronavirus activities of MPA and MMF

Virus	Cell	TC_{50} (μM)		IC_{50} (μM)		SI	
		MPA	MMF	MPA	MMF	MPA	MMF
HCoV-229E	Huh7	> 100 ± 0	> 100 ± 0	0.284 ± 0.22	0.165 ± 0.04	> 352.1	> 606.1
	Huh7.5	> 100 ± 0	> 100 ± 0	0.352 ± 0.07	0.131 ± 0.08	> 284.1	> 763.4
	RPMI-2650	> 100 ± 0	> 100 ± 0	0.162 ± 0.10	0.153 ± 0.06	> 617.3	> 653.6
HCoV-OC43	C3A	> 100 ± 0	> 100 ± 0	0.269 ± 0.22	0.638 ± 0.23	> 371.7	> 156.7
	H460	> 100 ± 0	> 100 ± 0	0.107 ± 0.07	0.232 ± 0.02	> 934.6	> 431.0
	RPMI-2650	> 100 ± 0	> 100 ± 0	0.104 ± 0.12	0.086 ± 0.10	> 961.5	> 1162.8

TC_{50} was determined by CCK assay and IC_{50} was determined by qRT-PCR ($n = 3$). The selectivity index (SI) was the quotient of TC_{50} and IC_{50}.

response (Supplementary Fig. 1), indicating that the anti-CoVs effect of MMF may not be mediated by interferon, as opposed to its reported anti-HCV mechanism [23].

Combinatorial effects of MMF and other antiviral compounds

Drug combination therapy is more commonly used in clinical treatments than monotherapy because it enhances the efficacy by targeting multiple stages of the pathogen's life cycle with lower dosages and prevents the possibility of drug resistance and the side effect associated of monotherapy [34]. The above results proved that as an immunosuppressive agent, MMF also processed promising antiviral activity. Accordingly, we speculated that the clinical usage of MMF can be expanded through drug combination. We chose several known viral or host replicase inhibitors for combination with MMF, including, the RdRp inhibitor molnupiravir, main protease inhibitor GC376 and cathepsin L inhibitor E64d. The indicated concentrations of all three drugs were added with MMF simultaneously during virus infection in HCoV-229E-infected Huh7.5 cells and HCoV-OC43-infected H460 cells. MMF and molnupiravir targeted the process of nucleotide metabolism as guanylate synthesis inhibitor and cytosine nucleoside analogue separately. Surprisingly, we discovered that the combination of MMF and molnupiravir had better effects (Fig. 6a, b). Main protease is highly conserved and indispensable to polyprotein cleavage in CoVs, and is a critical target for drug development [35, 36]. Main protease inhibitor GC376, which acted differently from host-targeting antiviral drug MMF, and as expected, they were combined more effectively (Fig. 6c, d). We also selected a promising patent drug target, the inhibitor of Cathepsin L. We hypothesized that E64d and MMF can inhibit the entry and replication stages of the virus separately and played a synergistic role. As shown in Fig. 6e, f, they produced a greater effect when combined than the sum of their individual effects, showing a synergistic effect. The inhibitory effect of MMF increased with increased concentration of E64d, and the inhibitory effect of E64d also increased with increased of MMF concentration. This finding indicated that MMF had significant value in combination therapy. Therefore, MMF was a promising candidate of combination therapy in CoVs inhibition and can open more doors for COVID-19 treatment.

Discussion

MMF and MPA are widely used in the routine treatment of organ transplantation and autoimmune diseases. Although it was reported that IMPDH inhibitors have limited inhibitory effects against SARS-CoV [37], after the outbreak of SARS-CoV-2, studies have shown that MMF and MPA have anti-SARS-CoV-2 activities [26, 27]. Our study showed that MMF and MPA had broad antiviral spectrum against CoVs including HCoV-229E, HCoV-OC43, and SARS-CoV-2 and various variants. Moreover, MMF exhibits synergistic effects with anti-CoV drugs/compounds with different mechanisms of action.

As an ester derivative, MMF is more lipid soluble and rapidly absorbed. It is converted into the active form MPA after oral administration. Our research showed there was little difference between MPA and MMF in antiviral efficacy at the cellular level. Therefore, in the future study of broad-spectrum antiviral efficacy, more attention should be paid to MMF with more clinical applications. Other derivatives such as mycophenolic acid methyl ester also have anti-IAV activity [38], indicating that with MPA as the parent nucleus, chemists can continuously modify other derivatives with higher bioavailability and lower toxicity to enrich the library of antiviral compounds. Additionally, MMF had a potent antiviral effect at 5 μM at the cellular level, lower than the plasma level used in clinical practice [39–41], suggesting that MMF can enrich the usage for people infected with CoVs.

Our results showed that the high concentration of 400 μM guanosine almost completely reversed the

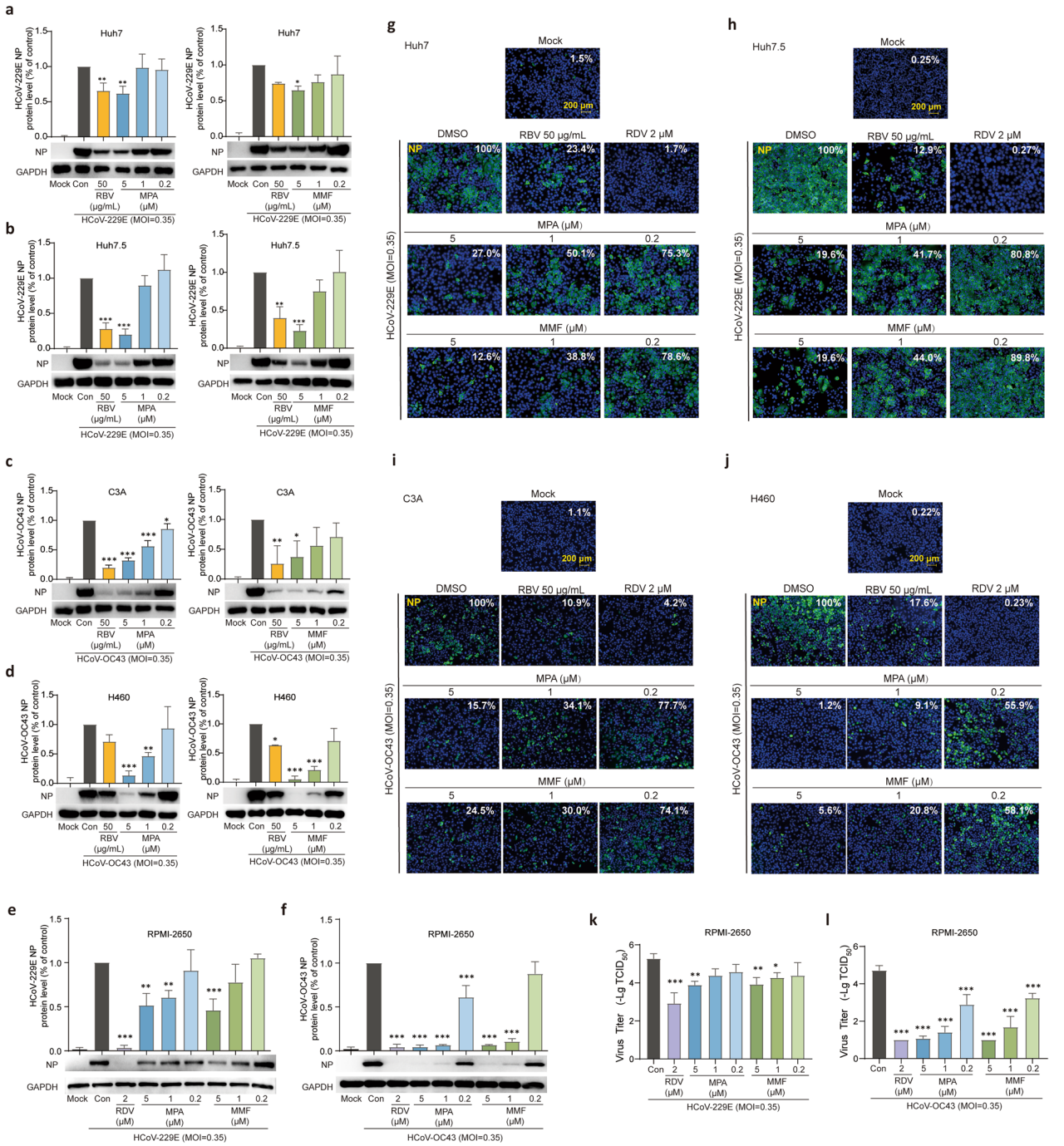

Fig. 3 MMF and MPA inhibited viral protein levels and viral yield of HCoV-229E and HCoV-OC43. Cells were infected with HCoV-229E (MOI = 0.35) or HCoV-OC43 (MOI = 0.35), and treated with different concentrations of MMF or MPA for 24 h. **a–f** The cells were harvested for western blotting assay ($n = 3$). $^{*}P < 0.05$, $^{**}P < 0.01$, $^{***}P < 0.001$ *vs.* virus control (Con), one-way ANOVA with Holm-Sidak multiple comparisons test. **g–j** The cells were fixed and NP was detected with immunofluorescence (IF) assay. Green particles represent NP and the blue ones represent cell nucleus. The quantitative study on immunofluorescence was comparison of the total fluorescence values of each experimental group with the control group and analyzed by Image J software. **k–l** Viral titers were detected by the 50% tissue culture infectious dose assay ($TCID_{50}$) ($n = 3$). $^{*}P < 0.05$, $^{**}P < 0.01$, $^{***}P < 0.001$ *vs.* virus control (Con), one-way ANOVA with Holm-Sidak multiple comparisons test

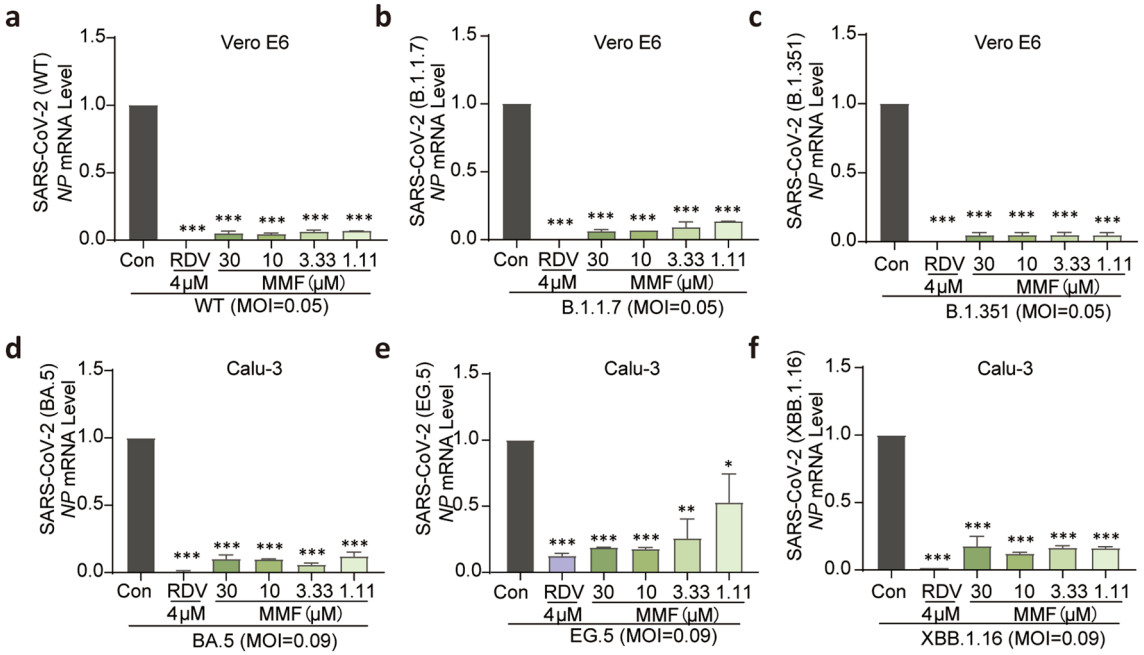

Fig. 4 MMF exerts strong inhibition activity against SARS-CoV-2 on mRNA levels. **a–c** Vero E6 cells were infected with SARS-CoV-2 WT and variants B.1.1.7 and B.1.351. **d–f** Calu-3 cells were infected with SARS-COV-2 variants BA.5, EG.5 and XBB.1.16. Indicated concentrations of MMF were added simultaneously and treated for 24 h and the *NP* mRNA levels was determined by qRT-PCR assay, relative quantification was performed and normalized to the housekeeping gene GAPDH ($n=3$). *$P<0.05$, **$P<0.01$, ***$P<0.001$ *vs.* virus control (Con), one-way ANOVA with Holm-Sidak multiple comparisons test

(See figure on next page.)

Fig. 5 The antiviral activity of MMF is achieved by non-competitive inhibition of the IMPDH enzyme. **a** Schematic diagram of time-of-addition assay. **b**, **c** Time-of-addition assay of MMF. Cells were seeded onto 96-well plates and infected with HCoV-229E or HCoV-OC43 (MOI = 3.5) for 1 h on ice. 5 μM MMF was added at different time points and cells were fixed at 9 h. Intracellular viral NP protein was detected with immunofluorescence (IF) assay. Green particles represent NP and the blue ones represent cell nucleus. The quantitative study on immunofluorescence was comparison of the total fluorescence values of each experimental group with the control group and analyzed by Image J software. **d**, **e** CETSA assay to detect the binding between IMPDH and MMF in the cell lysis of Huh7.5 and H460. Each lane represents the protein level of IMPDH at various temperatures after incubation with MMF or DMSO control, and relative density of IMPDH was normalized by the protein gray value at 47 °C ($n=3$). **f**, **g** Cells were infected with HCoV-229E (MOI = 0.35) or HCoV-OC43 (MOI = 0.35), and treated with different concentrations of guanosine and MMF for 24 h. The cells were harvested for western blotting assay ($n=3$). *$P<0.05$, **$P<0.01$, ***$P<0.001$ *vs.* virus control (Con) or $^{\#}P<0.05$, $^{\#\#}P<0.01$, $^{\#\#\#}P<0.001$ *vs.* MMF treated group (The third group), one-way ANOVA with Holm-Sidak multiple comparisons test

antiviral effect of MMF, indicating that its anti-CoVs activity depended on IMPDH inhibition, in line with that reported in literature for MMF against many other types of viruses. Interestingly, MMF has been reported to stimulate the expression of ISG such as interferon regulatory factor 1 to inhibit HCV [23], whereas our results suggest that the anti-CoVs activity of MMF is independent of the regulation of IFN. In addition, MMF was reported to suppress autophagy to inhibit dengue virus, as evidenced by decreased LC3B-II level and conversion of LC3B-I to LC3B-II, decreased autophagosome formation, and increased p62 level [24, 25]. MMF preconditioning was found to protect mouse liver against ischemia/reperfusion injury in WT and toll-like receptor 4 knockout mice, probably by decreasing apoptosis and the inflammatory response [42]. Therefore, the antiviral mechanisms of MMF and its effects on signaling pathways or immune environment warrant further study.

Optimizing the use of immunosuppressive agents alone may not eliminate viral infection, and it needs to be combined with other targeted antiviral drugs. MMF can positively synergize with molnupiravir, GC376, or E64d to inhibit HCoV-229E and HCoV-OC43. MPA can be combined with ETV to inhibit HBV, combined with oseltamivir to inhibit IAV, and combined with MTX or Tac to inhibit HADV [34, 43, 44], which also demonstrate

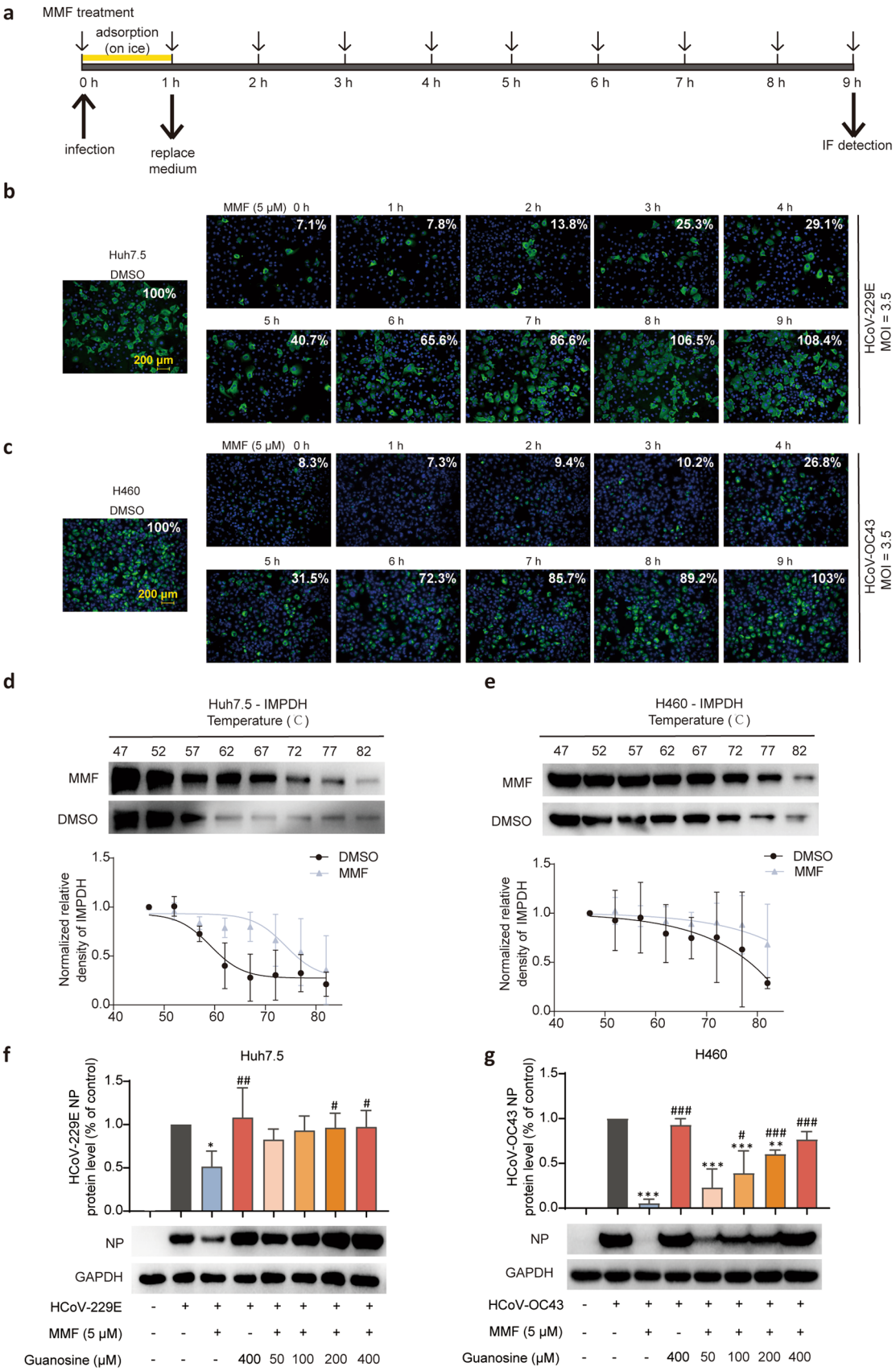

Fig. 5 (See legend on previous page.)

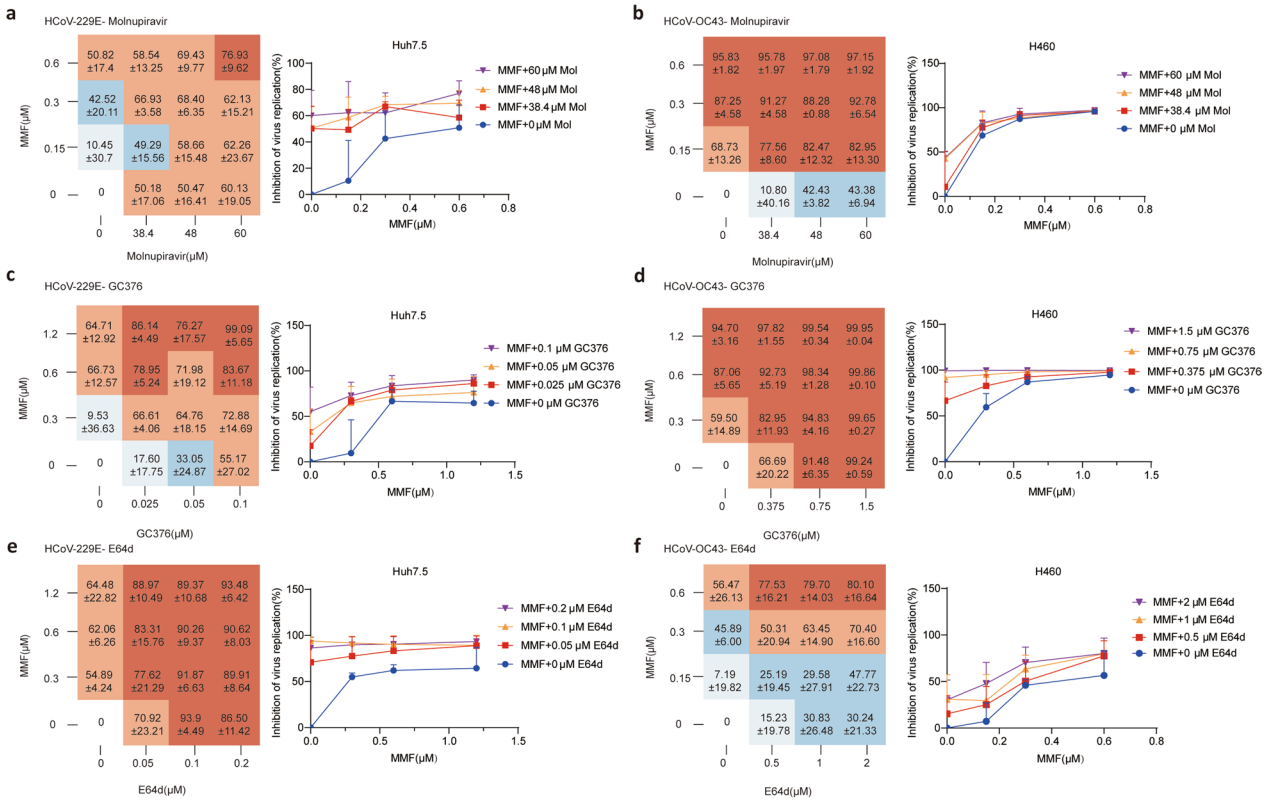

Fig. 6 Combinatorial effects of MMF and other antiviral compounds. **a**, **b** Dose–response matrixs and dose–response curves of combination of MMF and molnupiravir. **c**, **d** Dose–response matrixs and dose–response curves of combination of MMF and GC376. **e**, **f** Dose–response matrixs and dose–response curves of combination of MMF and E64d. In detail, Huh7.5 cells were infected with HCoV-229E (MOI = 0.35) for 24 h (a, c, e, $n = 3$, mean ± SD) and H460 cells were infected with HCoV-OC43 for 24 h (MOI = 0.35) (b, d, f, $n = 3$, mean ± SD). The horizontal and vertical coordinates of the dose–response matrix are the concentrations of the combined drugs. *NP* mRNA levels was determined by qRT-PCR assay and relative quantification. The inhibition of virus replication of non-administrated group was regarded as zero to calculate the inhibition of each administration group

its clinical combined potential. Combinations of MPA with molnupiravir and nirmatrelvir exerted an additive or synergistic anti-SARS-CoV-2 activity with ZIP values of 6.715 and 28.35 [45], consistent with our findings on the optimal management of immunocompromised patients infected with CoVs.

As widely used steroid-sparing immunosuppressant, the clinical significance of MMF/MPA for antiviral therapy purpose need to be further clarify. Since virus infection can trigger robust well-coordinated immune response to clear virus, or provoke self-intolerant immunopathological effects that exacerbate the disease.

Conclusion

MMF and MPA had inhibitory effects on a wide range of human CoVs, including SARS-CoV-2 ancestral strain and its variants. MMF and MPA can also bind with IMPDH protein and exerted antiviral activities through the non-competitive inhibition of it. Moreover, MMF had a synergistic antiviral effect when combined with other drugs, showing its potential clinical antiviral applications.

Abbreviations

MPA	Mycophenolic acid
MMF	Mycophenolate mofetil
CoV	Coronavirus
IMPDH	Inosine-5′-monophosphate dehydrogenase
Gua	Guanosine
RBV	Ribavirin
RDV	Remdesivir
Mol	Molnupiravir
E64d	Aloxistatin

Supplementary Information

The online version contains supplementary material available at https://doi.org/10.1186/s12985-025-02673-2.

Additional file1 (DOCX 16 KB)

Additional file2 (TIF 1001 KB)

Additional file3 (DOCX 3787 KB)

Acknowledgements
Not applicable.

Author contributions
MY Wu and K Wang performed all the experiments and drafted the manuscript. HQ Wang provided suggestions on the experimental design and helped edit the manuscript. HY Yan and S Wu performed the experiment of viral infection and analyzed experimental data. G Yang provides advice in this study. YH Li, YS Che and JD Jiang designed this study, and edited this manuscript. All authors read and approved the final manuscript.

Funding
This work was financially supported by National Natural Science Foundation of China (82003818, 82151525, 82394465 (82394460)) and CAMS Innovation Fund for Medical Sciences (2021-I2M-1-030, 2022-I2M-CoV19-001, China).

Availability of data and materials
No datasets were generated or analysed during the current study.

Declarations

Consent for publication
All authors consent to the publication of the manuscript.

Competing interests
The authors declare that they have no conflict of interests.
The authors declare no competing interests.

Animal and human rights statement
This article does not contain any studies with human or animal subjects performed by any of the authors.

Received: 22 October 2024 Accepted: 17 February 2025
Published online: 04 March 2025

References

1. The species severe acute respiratory syndrome-related coronavirus: classifying 2019-nCoV and naming it SARS-CoV-2. Nat Microbiol. 2020;5:536–544.
2. Khalil AM, Martinez-Sobrido L, Mostafa A. Zoonosis and zooanthroponosis of emerging respiratory viruses. Front Cell Infect Microbiol. 2023;13:1232772.
3. Maestri R, Perez-Lamarque B, Zhukova A, Morlon H. Recent evolutionary origin and localized diversity hotspots of mammalian coronaviruses. Elife. 2024;13:RP91745.
4. Saravolatz LD, Depcinski S, Sharma M. Molnupiravir and Nirmatrelvir-Ritonavir: oral coronavirus disease 2019 antiviral drugs. Clin Infect Dis. 2023;76:165–71.
5. Balik M, Waldauf P, Jurisinova I, Svobodova E, Diblickova M, Tencer T, Zavora J, Smela G, Kupidlovska L, Adamkova V, et al. SARS-CoV-2 viral load is linked to remdesivir efficacy in severe Covid-19 admitted to intensive care. Sci Rep. 2024;14:20825.
6. Zhang JL, Li YH, Wang LL, Liu HQ, Lu SY, Liu Y, Li K, Liu B, Li SY, Shao FM, et al. Azvudine is a thymus-homing anti-SARS-CoV-2 drug effective in treating COVID-19 patients. Signal Transduct Target Ther. 2021;6:414.
7. Harrigan SP, Velásquez García HA, Abdia Y, Wilton J, Prystajecky N, Tyson J, Fjell C, Hoang L, Kwong JC, Mishra S, et al. The clinical severity of COVID-19 variants of concern: retrospective population-based analysis. JMIR Public Health Surveill. 2024;10: e45513.
8. Jung H, Park JY, Yoon D, Kang DY, Jung J, Kim JH, Shin JY. Patient-reported adverse events among elderly patients receiving novel oral COVID-19 antivirals: a nationwide sampled survey in Korea. J Korean Med Sci. 2024;39: e270.
9. Lopez UM, Hasan MM, Havranek B, Islam SM. SARS-CoV-2 resistance to small molecule inhibitors. Curr Clin Microbiol Rep. 2024;11:127–39.
10. Bills GF, Gloer JB. Biologically active secondary metabolites from the fungi. Microbiol Spectr. 2016;4:10.
11. Tönshoff B. Immunosuppressants in organ transplantation. Handb Exp Pharmacol. 2020;261:441–69.
12. Bhat R, Tonutti A, Timilsina S, Selmi C, Gershwin ME. Perspectives on mycophenolate mofetil in the management of autoimmunity. Clin Rev Allergy Immunol. 2023;65:86–100.
13. You Y, Zhou Z, Wang F, Li J, Liu H, Cheng X, Su Y, Chen X, Zheng H, Sun Y, et al. Mycophenolate mofetil and new-onset systemic lupus erythematosus: a randomized clinical trial. JAMA Netw Open. 2024;7: e2432131.
14. Allison AC, Eugui EM. Purine metabolism and immunosuppressive effects of mycophenolate mofetil (MMF). Clin Transpl. 1996;10:77–84.
15. Qiu Y, Fairbanks LD, Rückermann K, Hawrlowicz CM, Richards DF, Kirschbaum B, Simmonds HA. Mycophenolic acid-induced GTP depletion also affects ATP and pyrimidine synthesis in mitogen-stimulated primary human T-lymphocytes. Transplantation. 2000;69:890–7.
16. Morales Vasquez D, Park JG, Ávila-Pérez G, Nogales A, de la Torre JC, Almazan F, Martinez-Sobrido L. Identification of inhibitors of ZIKV replication. Viruses. 2020;12:1041.
17. Padalko E, Verbeken E, Matthys P, Aerts JL, De Clercq E, Neyts J. Mycophenolate mofetil inhibits the development of Coxsackie B3-virus-induced myocarditis in mice. BMC Microbiol. 2003;3:25.
18. Hishiki T, Morita T, Akazawa D, Ohashi H, Park ES, Kataoka M, Mifune J, Shionoya K, Tsuchimoto K, Ojima S, et al. Identification of IMP dehydrogenase as a potential target for anti-Mpox virus agents. Microbiol Spectr. 2023;11: e0056623.
19. Hart BJ, Dyall J, Postnikova E, Zhou H, Kindrachuk J, Johnson RF, Olinger GG, Frieman MB, Holbrook MR, Jahrling PB, Hensley L. Interferon-β and mycophenolic acid are potent inhibitors of Middle East respiratory syndrome coronavirus in cell-based assays. J Gen Virol. 2014;95:571–7.
20. Takhampunya R, Ubol S, Houng HS, Cameron CE, Padmanabhan R. Inhibition of dengue virus replication by mycophenolic acid and ribavirin. J Gen Virol. 2006;87:1947–52.
21. Park JG, Ávila-Pérez G, Nogales A, Blanco-Lobo P, de la Torre JC, Martínez-Sobrido L. Identification and characterization of novel compounds with broad-spectrum antiviral activity against influenza A and B viruses. J Virol. 2020;94:10.
22. Chang QY, Guo FC, Li XR, Zhou JH, Cai X, Pan Q, Ma XX. The IMPDH inhibitors, ribavirin and mycophenolic acid, inhibit peste des petits ruminants virus infection. Vet Res Commun. 2018;42:309–13.
23. Pan Q, de Ruiter PE, Metselaar HJ, Kwekkeboom J, de Jonge J, Tilanus HW, Janssen HL, van der Laan LJ. Mycophenolic acid augments interferon-stimulated gene expression and inhibits hepatitis C Virus infection in vitro and in vivo. Hepatology. 2012;55:1673–83.
24. Manchala NR, Dungdung R, Trivedi P, Unniyampurath U, Pilankatta R. Mycophenolic acid (MPA) modulates host cellular autophagy progression in sub genomic dengue virus-2 replicon cells. Microb Pathog. 2019;137: 103762.
25. Fang S, Su J, Liang B, Li X, Li Y, Jiang J, Huang J, Zhou B, Ning C, Li J, et al. Suppression of autophagy by mycophenolic acid contributes to inhibition of HCV replication in human hepatoma cells. Sci Rep. 2017;7:44039.
26. Kato F, Matsuyama S, Kawase M, Hishiki T, Katoh H, Takeda M. Antiviral activities of mycophenolic acid and IMD-0354 against SARS-CoV-2. Microbiol Immunol. 2020;64:635–9.
27. Volle R, Murer L, Petkidis A, Andriasyan V, Savi A, Bircher C, Meili N, Fischer L, Sequeira DP, Mark DK, et al. Methylene blue, Mycophenolic acid, Posaconazole, and Niclosamide inhibit SARS-CoV-2 Omicron variant BA.1 infection of human airway epithelial organoids. Curr Res Microb Sci. 2022;3:100158.
28. Li H, Li J, Li J, Li H, Wang X, Jiang J, Lei L, Sun H, Tang M, Dong B, et al. Carrimycin inhibits coronavirus replication by decreasing the efficiency of programmed -1 ribosomal frameshifting through directly binding to the RNA pseudoknot of viral frameshift-stimulatory element. Acta Pharm Sin B. 2024;14:2567–80.
29. Wang Y, Zhan Y, Xu R, Shao R, Jiang J, Wang Z. Src mediates extracellular signal-regulated kinase 1/2 activation and autophagic cell death induced by cardiac glycosides in human non-small cell lung cancer cell lines. Mol Carcinog. 2015;54(Suppl 1):E26-34.
30. Yan H, Sun J, Wang K, Wang H, Wu S, Bao L, He W, Wang D, Zhu A, Zhang T, et al. Repurposing carrimycin as an antiviral agent against human coronaviruses, including the currently pandemic SARS-CoV-2. Acta Pharm Sin B. 2021;11:2850–8.

31. Zhao X, Zheng S, Chen D, Zheng M, Li X, Li G, Lin H, Chang J, Zeng H, Guo JT. LY6E restricts entry of human coronaviruses, including currently pandemic SARS-CoV-2. J Virol. 2020;94:10.
32. Reed LJ, Muench H. A simple method of estimating fifty per cent endpoints12. Am J Epidemiol. 1938;27:493–7.
33. El-Maradny YA, Badawy MA, Mohamed KI, Ragab RF, Moharm HM, Abdallah NA, Elgammal EM, Rubio-Casillas A, Uversky VN, Redwan EM. Unraveling the role of the nucleocapsid protein in SARS-CoV-2 pathogenesis: From viral life cycle to vaccine development. Int J Biol Macromol. 2024;279: 135201.
34. Ying C, Colonno R, De Clercq E, Neyts J. Ribavirin and mycophenolic acid markedly potentiate the anti-hepatitis B virus activity of entecavir. Antiviral Res. 2007;73:192–6.
35. Yang X, Chen X, Bian G, Tu J, Xing Y, Wang Y, Chen Z. Proteolytic processing, deubiquitinase and interferon antagonist activities of Middle East respiratory syndrome coronavirus papain-like protease. J Gen Virol. 2014;95:614–26.
36. Jorda A, Ensle D, Eser H, Glötzl F, Riedl B, Szell M, Valipour A, Zoufaly A, Wenisch C, Haider D, et al. Real-world effectiveness of nirmatrelvir-ritonavir and molnupiravir in non-hospitalized adults with COVID-19: a population-based, retrospective cohort study. Clin Microbiol Infect. 2024.
37. Barnard DL, Day CW, Bailey K, Heiner M, Montgomery R, Lauridsen L, Winslow S, Hoopes J, Li JK, Lee J, et al. Enhancement of the infectivity of SARS-CoV in BALB/c mice by IMP dehydrogenase inhibitors, including ribavirin. Antiviral Res. 2006;71:53–63.
38. Wang Z, Sun L, Zhao H, Sow MD, Zhang Y, Wang W. Inhibition effects and mechanisms of marine compound mycophenolic acid methyl ester against influenza A virus. Mar Drugs. 2024;22:190.
39. Dasgupta A. Therapeutic drug monitoring of mycophenolic acid. Adv Clin Chem. 2016;76:165–84.
40. Doki K, Yoshida K, Usui J, Takahashi K, Oda T, Yamagata K, Homma M. External validation of a limited sampling strategy for the estimation of mycophenolic acid exposure between different assay methods: PETINIA and HPLC methods. Clin Transpl. 2024;38: e15471.
41. Liu R, Wu Q, Wu C, Qu Y, Fang Y, De J, Fan R, Song W. Metabolic signatures of metabolites of the purine degradation pathway in human plasma using HILIC UHPLC-HRMS. J Pharm Biomed Anal. 2024;251: 116451.
42. Xiong C, Du Z, Zhu Y, Xue M, Jiang Y, Zhong Y, Jiang L, Chen H, Shi M. Mycophenolate mofetil preconditioning protects mouse liver against ischemia/reperfusion injury in wild type and toll-like receptor 4 knockout mice. Transpl Immunol. 2021;65: 101357.
43. Wang X, Pu F, Yang X, Feng X, Zhang J, Duan K, Nian X, Ma Z, Ma XX, Yang XM. Immunosuppressants exert antiviral effects against influenza A(H1N1)pdm09 virus via inhibition of nucleic acid synthesis, mRNA splicing, and protein stability. Virulence. 2024;15:2301242.
44. Carretero-Ledesma M, Aguilar-Guisado M, Berastegui-Cabrera J, Balsera-Manzanero M, Pachón J, Cordero E, Sánchez-Céspedes J. Antiviral activity of immunosuppressors alone and in combination against human adenovirus and cytomegalovirus. Int J Antimicrob Agents. 2024;63: 107116.
45. Wang Y, Li P, Lavrijsen M, Rottier RJ, den Hoed CM, Bruno MJ, Kamar N, Peppelenbosch MP, de Vries AC, Pan Q. Immunosuppressants exert differential effects on pan-coronavirus infection and distinct combinatory antiviral activity with molnupiravir and nirmatrelvir. United Eur Gastroenterol J. 2023;11:431–47.

Publisher's Note